Received: 1 November 2023 | Accepted: 7 December 2023

DOI: 10.1111/1759-7714.15196

ORIGINAL ARTICLE

WILEY

TPI1 promotes MAPK/ERK-induced EMT, cell migration and invasion in lung adenocarcinoma

Yu Li[1,2] | Bin Pan[1,3] | Feiyang Zhang[4] | Xinyu Jia[1,2] | Xinyu Zhu[1,2] | Xin Tong[1,2] | Jun Zhao[1,2] | Chang Li[1,2]

[1]Department of Thoracic Surgery, The First Affiliated Hospital of Soochow University, Suzhou, China

[2]Institute of Thoracic Surgery, The First Affiliated Hospital of Soochow University, Suzhou, China

[3]Department of Cardiothoracic Surgery, People's Hospital Affiliated to Jiangsu University, Zhenjiang, China

[4]Soochow University Medical College, Suzhou, China

Correspondence
Xin Tong, Jun Zhao, and Chang Li, Department of Thoracic Surgery, The First Affiliated Hospital of Soochow University, Suzhou, 215006, China.
Email: txin@suda.edu.cn; junzhao@suda.edu.cn; cli@suda.edu.cn

Funding information
National Natural Science Foundation of China, Grant/Award Number: 81873417; Soochow University Extracurricular Academic, Grant/Award Number: KY2023016Z

Abstract

Background: Triosephosphate isomerase 1 (TPI1), as a widely involved glycolytic enzyme, plays a significant role in glucose metabolism and is highly expressed in various tumors. However, its role in lung adenocarcinoma (LUAD) remains incompletely understood.

Methods: Through bioinformatic analysis, we identified a positive association between high expression of TPI1 and metastasis in LUAD. Western blot, RT-qPCR, wound healing assays and transwell experiments, were employed to investigate potential mechanisms.

Results: In this study, bioinformatic analysis showed that high expression of TPI1 was associated with poor prognosis in LUAD patients. We examined the expression of TPI1 in 29 paired LUAD tissues and found that TPI1 expression was higher in LUAD tissues than in paired adjacent noncancerous tissues. Meanwhile, overexpression of TPI1 promoted the epithelial-mesenchymal transition (EMT) process in LUAD cells, while silencing TPI1 weakened the EMT process. Furthermore, TPI1 was shown to regulate EMT through the MAPK/ERK signaling pathway.

Conclusion: TPI1 promotes LUAD metastasis by activating the MAPK/ERK signaling pathway.

KEYWORDS
TPI1, LUAD, EMT, MAPK/ERK

INTRODUCTION

Lung cancer is one of the most common cancers globally,[1,2] with approximately 85% of cases classified as non-small cell lung cancer (NSCLC). NSCLC subtypes include lung squamous cell carcinoma (LUSC), lung adenocarcinoma (LUAD) and large cell lung carcinoma. LUAD is the predominant subtype, accounting for approximately 40% of all lung cancer cases.[3] Distant metastasis of cancer cells contributes to the poor prognosis in lung cancer patients,[4] wherein tumor cells gradually spread from the primary tumor through the bloodstream, lymphatic system, or other pathways. In this process, epithelial-mesenchymal transition (EMT) has emerged as a key process linked to tumor metastasis.[5,6]

When cells undergo EMT, the expression of epithelial markers decreases while that of mesenchymal markers increases.[7] This shift weakens cell–cell adhesion and promotes cell migration. Several signaling pathways,[8–10] including the mitogen-activated protein kinase (MAPK) pathway, have been shown to regulate EMT, through the phosphorylation and activation of specific transcription factors such as activator protein 1 (AP-1) and c-Jun, which regulate EMT inducers such as Snail, Slug, and ZEB, thus facilitating occurrence and progression of EMT.[11–13]

Triosephosphate isomerase (TPI1) plays a crucial role in the glycolytic pathway, facilitating the rapid conversion between dihydroxyacetone phosphate and 3-phosphoglyceraldehyde.[14,15]

Yu Li, Bin Pan and Feiyang Zhang contributed equally to this study.

Notably, TPI1 expression levels vary across different tumors. High TPI1 expression is observed in breast cancer,[16] stomach cancer,[17] and colon cancer,[18] whereas it is low in hepatocellular carcinoma.[19,20] In hepatocellular carcinoma clinical samples, TPI1 expression significantly decreases compared to paired normal tissue, correlating with poorer overall survival, larger tumors, and higher metastasis rates.[20] Conversely, TPI1 is overexpressed in breast cancer, and activates the PI3K/AKT/mTOR pathway, further facilitating EMT mediated by cell division cycle-associated 5 (CDCA5).[16] Moreover, TPI1 is highly expressed in serum samples from individuals with lung cancer, highlighting its diverse roles in different tumors.[21] The aim of this study was to clarify the function of TPI1 in LUAD development, particularly in cancer metastasis.

METHODS

Gene expression analysis

Data of RNA expression and clinicopathological information were downloaded from The Cancer Genome Atlas (TCGA) and GTEx datasets via the UCSC Xena database (https://xenabrowser.net/datapages/).[22]

Kaplan–Meier plotter database

We evaluated the prognostic relevance of TPI1 in lung cancer using the Kaplan–Meier plotter (https://kmplot.com/analysis/), an online database comprising data from 1925 clinical lung cancer patients, including 719 with LUAD.[22] Patients were stratified into high and low expression groups based on the median TPI1 levels. We then analyzed overall survival (OS) and first progression (FP) survival employing hazard ratios (HRs) with 95% confidence intervals (CIs) and log-rank *p*-values.

GO, KEGG pathway enrichment analyses and GSEA

The biological role of TPI1 in LUAD was analyzed through gene ontology (GO) and Kyoto Encyclopedia of Genes and Genomes (KEGG) enrichment analyses.[23] Gene set enrichment analysis (GSEA) was employed to assess significant differences in a predefined gene set between two biological states.[24] We conducted KEGG analyses using the R package Cluster Profiler and GSEA was executed using GSEA software version 4.1.0.

Cell lines and cell culture

The Cell Bank of Chinese Academy of Sciences provided the following cell lines: BEAS-2B, A549, H1650, H358, H1299, and 293 T. 293 T cells were grown in Dulbecco's modified Eagle medium (DMEM) supplemented with high glucose medium (Basal Media) containing 10% fetal bovine serum (FBS: ABW), while the remaining cells were cultured in RPMI 1640 medium (Basal Media) supplemented with 10% FBS (ABW) at a temperature of 37°C in a humidified incubator with 5% CO_2. MedChemExpress was the source of PD98059 and epidermal growth factor (EGF).

Human LUAD tissue samples

We collected 29 fresh-frozen LUAD tissues and paired normal tissues from patients who provided informed consent at the First Affiliated Hospital of Soochow University in Suzhou, China. All LUAD patients underwent pathological diagnosis and evaluation in accordance with the revised International System for Staging Lung Cancer. This research was conducted with approval from the Ethics Committee of Soochow University, and patient information is detailed in Table A1.

RNA extraction and qRT–PCR assays

The FastPure cell/tissue total RNA isolation kit (Vazyme) was used to extract total RNA from cells or tissues following the standard protocol. The synthesis of cDNA was performed using HiScript II reverse transcriptase from Vazyme. ACTB was used to normalize the mRNA expression levels of TPI1, FAS, RAF1, SOS2, BRAF, KRAS, ELK4, MAPK1, MET, RAC3, and MAPK12. The ΔΔCt method was used to determine the relative expression of each mRNA, with the quantitative reverse transcription- polymerase chain reaction (qRT–PCR) assay primers listed in Table A2.

Western blot assay

The cells were lysed using a combination of radioimmunoprecipitation assay (RIPA) lysis buffer, protease inhibitors, and phosphatase inhibitors. The protein samples were combined with loading buffer and dithiothreitol (DTT), followed by heating at a temperature of 100°C for a duration of 10 min. Afterward, the proteins were separated based on their size using an SDS-PAGE gel and then transferred onto a nitrocellulose membrane. To obstruct the membrane, a solution of 5% bovine serum albumin (BSA) was applied at room temperature for 1 h, and then the primary antibody was incubated overnight at 4°C. Following that, the membranes underwent three washes with tris-buffered saline (TBST) buffer prior to being incubated with a secondary antibody conjugated with horseradish peroxidase (HRP) at room temperature for a duration of 2 h. The membranes were rinsed three times with TBST buffer once more. Ultimately, protein identification was conducted utilizing an enhanced chemiluminescence (ECL) kit. The primary antibodies used in this study were rabbit anti-TPI1

(ABclonal), rabbit anti-extracellular regulated kinase (anti-ERK) (ABclonal), rabbit anti-p-ERK (ABclonal), mouse anti-E-cadherin (BD), mouse anti-N-cadherin (BD), mouse anti-vimentin (CST), mouse anti-Snail (CST), mouse anti-α-tubulin (ABclonal), and rabbit anti-β-actin (ABclonal). Additionally, HRP-conjugated secondary antibodies used were goat anti-rabbit (ABclonal) and goat anti-mouse (ABclonal).

Construction and acquisition of plasmids

The CDS sequence of TPI1 (NCBI no.: NM_000365.6) was downloaded from NCBI, and corresponding primers were designed for PCR amplification to obtain DNA fragment. DNA fragment was inserted into the pCDH-CMV-GFP-PURO-HA lentiviral vector, which had been previously cut with the endonucleases *BamH1*/*XbaI1* (NEB, UK). After mixing the plasmid with competent cells in a microcentrifuge tube they were incubated on ice for 30 min. The tube was then placed in a 42°C water bath for exactly 90 s and then returned immediately to the ice for 2 min. Prewarmed LB medium without antibiotics was then added to the tube which was incubated in a shaking incubator set at 37°C for 1 h. After incubation, the entire contents of the tube were spread evenly onto a luria broth (LB) agar plate with 100 μg/mL ampicillin (Solarbio Lifesciences). The plate was incubated overnight at 37°C. The next day, a single, well-isolated bacterial colony was selected from the plate using a pipette tip. A liquid LB culture containing 100 μg/mL ampicillin was incubated with the selected colony in a shaking incubator at 37°C for 12–14 h or until the culture reaches an optical density (OD) of approximately 1–1.2. The target DNA in the transformed E. coli were confirmed by Sanger sequencing, the plasmid was obtained by using the Axygen Plasmid Miniprep kit (Axygen). sh-RNA were directly synthesized (TsingKe), and the corresponding sequences are listed in Table A2.

Generation of stable cell lines

293 T cells were plated before transfection to achieve 70%–80% confluence. Then, 8.8 μg of psPAX2, 1.1 μg of pMD2. G, and 10 μg of the lentiviral vector were mixed in a tube with 500 μL DMEM with high glucose medium. In another separate tube, 40 μL lipo2000 (Thermo Fisher Scientific) was diluted with 500 μL DMEM with high glucose medium. The diluted lipo2000 was mixed with the plasmid mixture, gently combined, and then incubated at room temperature for 15 min before adding the transfection mixture dropwise to the 293 T cells. The cells were incubated in a 5% CO_2 incubator at 37°C for 48 h. After incubation, we collected the cell culture and it was centrifuged at 500 × g for 5–10 min. The clarified supernatant was passed through a sterile 0.45 μm syringe filter to eliminate any residual cellular debris. The A549 and H1299 cells were plated at 20%–30% confluence before adding the filtered lentivirus-containing supernatant and 4–8 μg/mL polybrene. After incubating the cells with the lentivirus at 37°C in a CO_2 incubator for 24–48 h, the culture medium was replaced with fresh medium containing 2 μg/mL puromycin (Solarbio Lifesciences) to incubate the cells.

Transwell migration and invasion assays

The experiments were carried out using Corning transwell plates. The upper chamber of the Transwell plates contained a total of 200 000 cells, categorized into migration and invasion groups depending on the presence of Matrigel coating. In the upper chamber, there was a culture medium containing 1% FBS, while the lower chamber was filled with 20% FBS serving as a chemoattractant. The cells were then placed in an incubator and left to incubate for a period of 24 h. Following the incubation period, the cells present in the upper chamber were eliminated, while the cells that had undergone migration or invasion were treated with methanol for a duration of 30 min and subsequently stained using a 1% crystal violet solution. Finally, by randomly choosing three small areas, the number of cells that had migrated or invaded was determined.

Wound-healing migration assay

Cells were plated in six-well plates. When the cell density reached around 80%–90%, the medium was replaced with serum-free culture medium. After carefully scraping the monolayer of cells using a sterilized pipette tip, three random fields were chosen and marked under a microscope and photographs were taken for documentation. Following 24 h of incubation in the cell incubator, photographs were captured again of the previously marked three fields. The width of the scratches was measured by ImageJ Launcher software.

RNA-seq analysis

Total RNA was isolated and purified using TRIzol reagent (Invitrogen). The Illumina Hiseq 4000 (LC Bio) was used to analyze the mRNA expression profiles of two distinct A549 cell groups: the TPI1-silenced (sh-TPI1-1) A549 cells and the control A549 cells (sh-NC).

Statistical analysis

The data are shown as mean ± standard deviation (SD), and statistical comparisons were performed using the student's *t*-test. The importance of patient sample data was evaluated by conducting Pearson's correlation coefficient testing or paired *t*-tests. p-values < 0.05 were considered statistically significant. Statistical analyses were conducted using GraphPad Prism 7 software (GraphPad).

RESULTS

High expression of TPI1 is positively associated with poor prognosis of LUAD patients

The overall expression profile of TPI1 was analyzed in the Cancer Genome Atlas (TCGA)-Genotype-Tissue Expression (GTEx) pan-cancer database and TPI1 showed widespread overexpression, suggesting its potential oncogenic role in most tumors, including lung cancer (Figure 1a). Further analysis within the TCGA database revealed overexpression of TPI1 in LUAD and LUSC (Figure 1b,c). However, TPI1 expression was associated with the prognosis in LUAD (Figure 1d), not LUSC patients (Figure 1e).

Identification of TPI1 expression in LUAD tissues

To validate the data from the TCGA database data, we collected 29 paired tissues which had been pathologically defined as LUAD. We analyzed the protein and mRNA

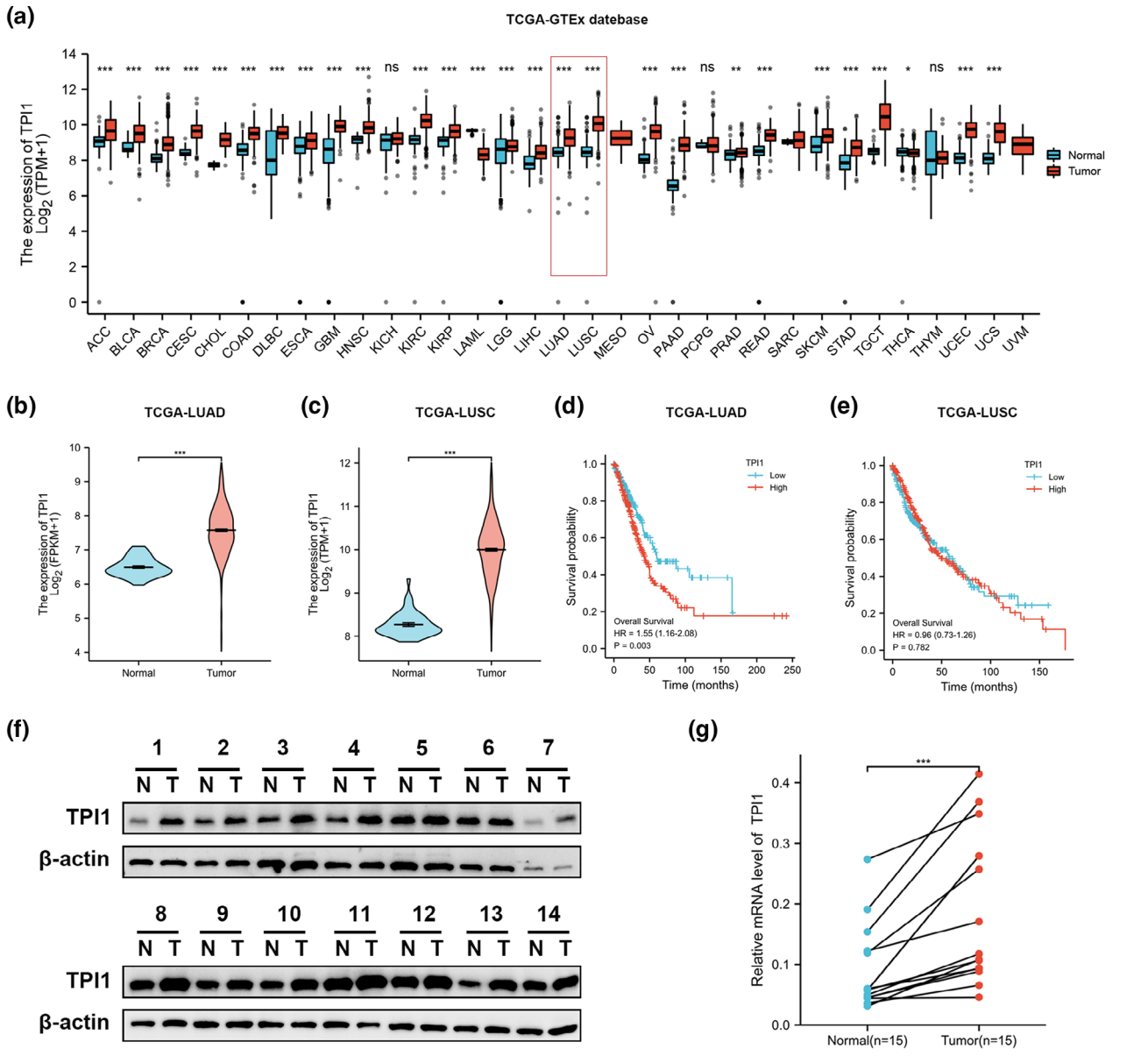

FIGURE 1 High expression of triosephosphate isomerase 1 (TPI1) is positively associated with poor prognosis of lung adenocarcinoma (LUAD) patients. (a) The expression of TPI1 in different types of cancers was investigated in the TCGA-GTEx database. (b, c) Increased expression of TPI1 in LUAD and lung squamous cell carcinoma (LUSC) compared to normal tissues in the cancer genome atlas (TCGA) database. (d, e) Kaplan–Meier survival curves showed the impact of CST1 on overall survival (OS) in LUAD and LUSC patients. (f, g) Comparison of TPI1 protein (14 pairs) and mRNA (15 pairs) expression between normal lung tissues and LUAD tissues. β-actin was used as an internal control.

expression levels of TPI1 in LUAD and paired adjacent non-cancerous tissue, which showed a widespread overexpression of TPI1 in LUAD (Figure 1f,g).

Bioinformatic analysis of TPI1 promotes LUAD metastasis

Analysis from the TCGA database suggested that the mRNA level of TPI1 was associated with tumor pathology and TNM stage (Figure 2a–d), suggesting that increased TPI1 expression may promote proliferation and migration of LUAD. In addition, Yuan et al. reported that TPI1 promotes the proliferation of LUAD cells.[25] Meanwhile, migration is one of the main reasons for poor prognosis in lung adenocarcinoma patients, and we concentrated on exploring the relationship between TPI1 overexpression and migration in LUAD. Upregulation of TPI1 in tumor tissues from individuals with LUAD was reproduced in four LUAD cell lines (A549, H358, H1650, and H1299), and compared to normal human bronchial epithelial cells (BEAS-2b), TPI1 was increased in both the protein and mRNA levels (Figure 2e) and stable TPI1-silenced A549 and H1299 cell lines by using the lentiviral system (Figure 2g).

Upregulated TPI1 promotes EMT, migration and invasion of LUAD cells

We established stable TPI1-overexpressing A549 and H1299 cell lines (Figure 3a). In TPI1-overexpressing A549 and H1299 cells, the expression of the epithelial marker E-cadherin decreased, while the mesenchymal markers N-cadherin, vimentin, and Snail increased (Figure 3b,c). Wound healing assays (Figure 3d,e) and transwell assays (Figure 3f,g) showed that overexpression TPI1 enhanced the migration and invasion of A549 and H1299 cells.

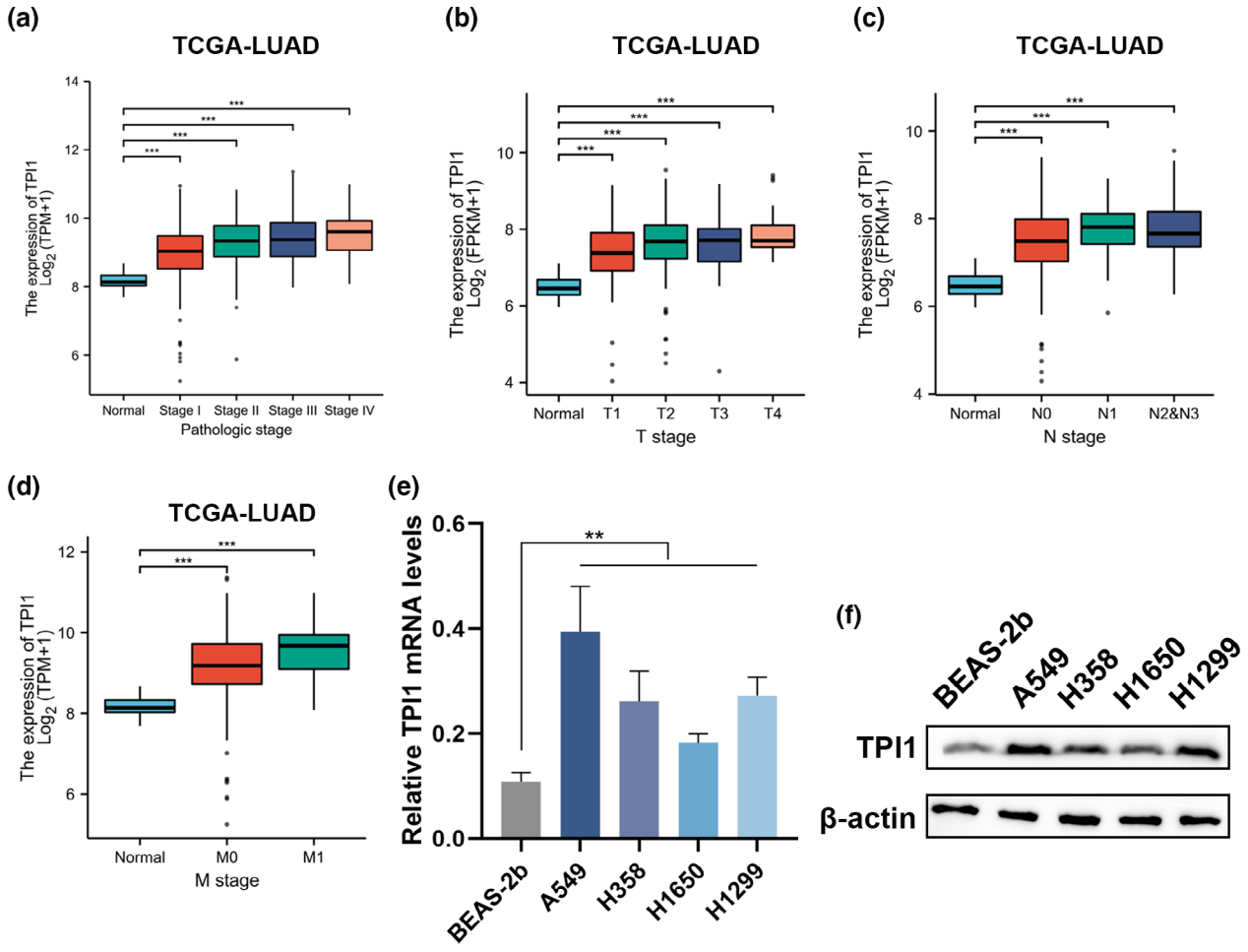

FIGURE 2 Bioinformatic analysis of triosephosphate isomerase 1 (TPI1) promotes lung adenocarcinoma (LUAD) metastasis. (a–d) The expression of TPI1 in different pathological stages and TNM stages in the Cancer Genome Atlas (TCGA) database. *$p < 0.05$, **$p < 0.01$, and ***$p < 0.001$. (e) Quantitative reverse transcription- polymerase chain reaction (qRT–PCR) and Western blot (WB) analysis of endogenous mRNA and protein levels of TPI1 in human bronchial epithelial cell line BEAS-2B, LUAD cell lines A549, H1299, H1650 and H358. (g) qRT-PCR and WB analyses of TPI1 expression levels in TPI1-silenced or control A549 and H1299 cells, which were transfected with short hairpin RNA (shRNA; sh-TPI1) or a scrambled sequence (sh-NC), β-actin was used as an internal control.

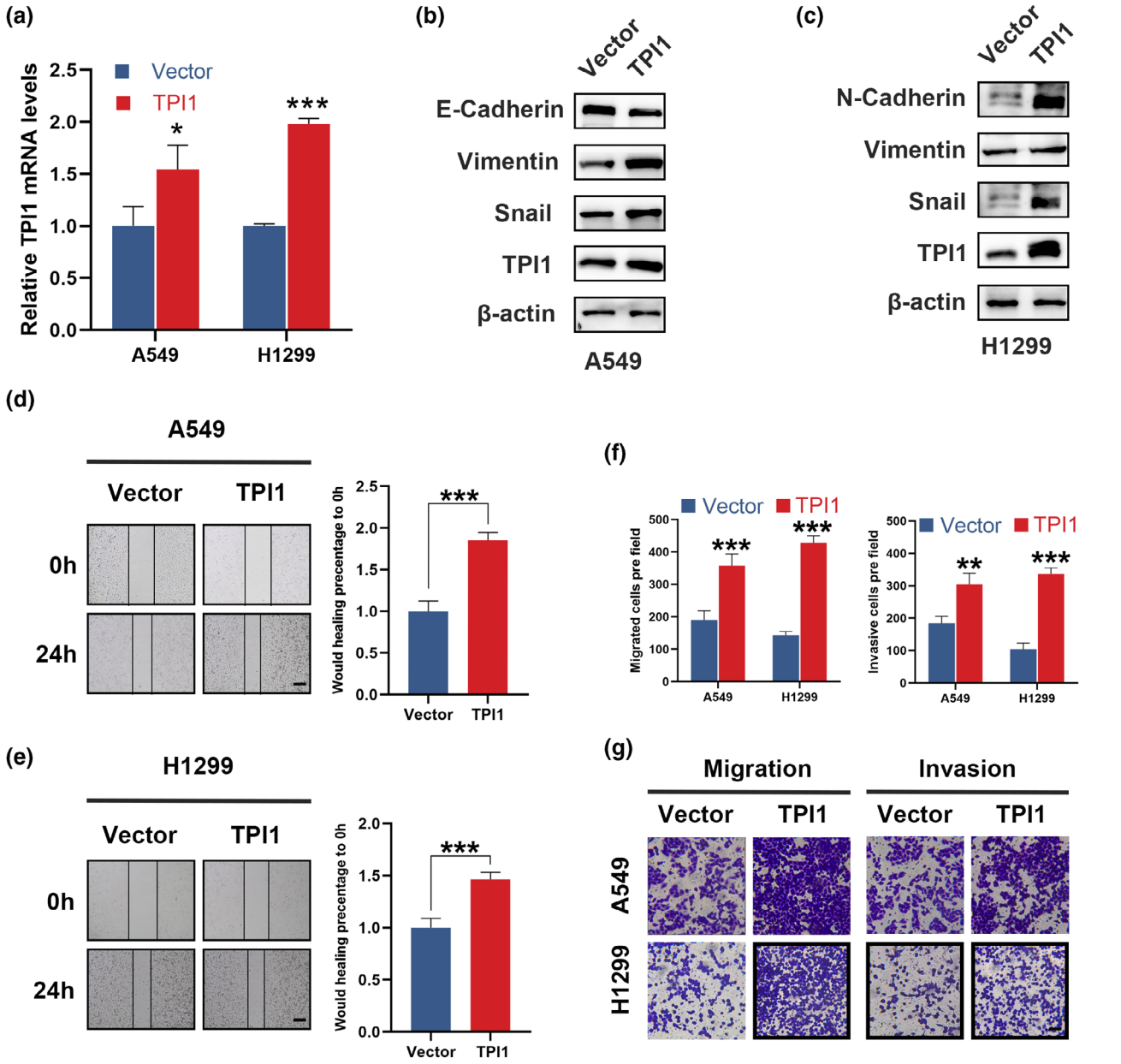

FIGURE 3 Upregulated triosephosphate isomerase 1 (TPI1) promotes epithelial-mesenchymal transition (EMT), migration and invasion of lung adenocarcinoma (LUAD) cells. (a) Quantitative reverse transcription- polymerase chain reaction (qRT-PCR) analyses of TPI1 expression levels in A549 and H1299 cells stably overexpressing TPI1. β-actin was used as an internal control. (b, c) Western blot analysis of TPI1, the EMT markers E-cadherin, N-cadherin, vimentin and Snail expressed in TPI1-overexpressing A549 and H1299 cells. (d, e) Wound healing assays of cell migration in TPI1-overexpressing or control A549 and H1299 cells. Wound healing was recorded and quantitated for at least three microscopic fields. Scale bar, 200 mm. Data are shown as the mean ± SD ($n = 3$). (f, g) TPI1-overexpressing A549 and H1299 cells were allowed to migrate through an 8-mm pore membrane or invade through a Matrigel-coated membrane in transwells. After 48 h, migrated and invasive cells were stained, photographed, and counted in at least three microscopic fields. Scale bar, 100 mm. Data are shown as the mean ± SD ($n = 3$).

Downregulated TPI1 suppresses EMT, migration and invasion of LUAD cells

Conversely, we established stable TPI1-overexpressing A549 and H1299 cell lines (Figure 4a). In TPI1-silenced A549 and H1299 cells, E-cadherin expression increased, while the expression of N-cadherin, vimentin, and Snail decreased (Figure 4b,c). Wound healing (Figure 3d,e) and transwell assays (Figure 3f,g) indicated that TPI1 silencing significantly inhibited the migration and invasion of A549 and H1299 cells.

RNA-seq analysis of TPI1 associated with the MAPK signaling pathway

We performed a gene set enrichment analysis (GSEA) on the transcriptome data of sh-NC and sh-TPI1-1 of A549

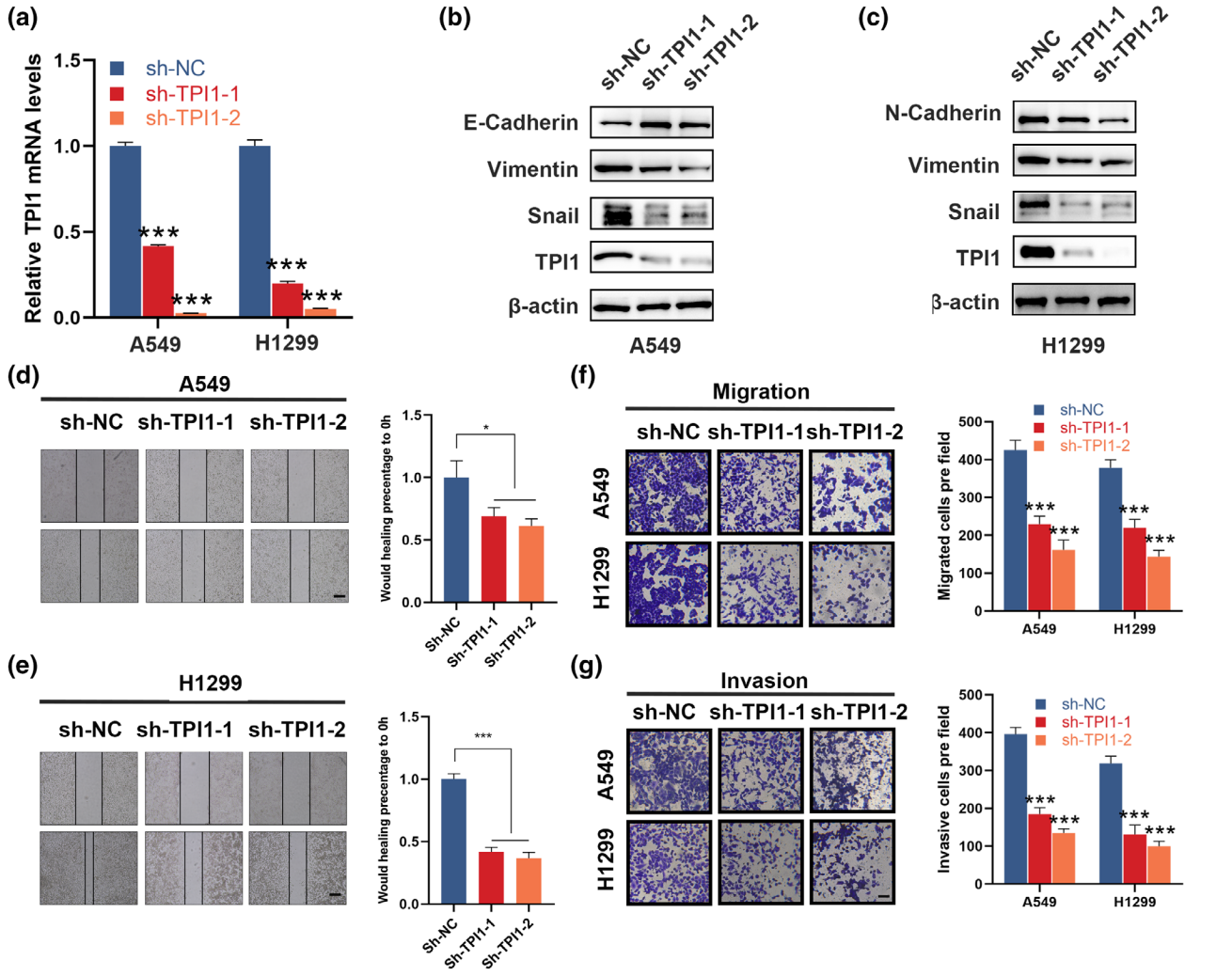

FIGURE 4 Downregulated triosephosphate isomerase 1 (TPI1) suppresses epithelial-mesenchymal transition (EMT), migration and invasion of lung adenocarcinoma (LUAD) cells. (a) Quantitative reverse transcription- polymerase chain reaction (qRT-PCR) and Western blot (WB) analyses TPI1 expression levels in TPI1-silenced or control A549 and H1299 cells, which were transfected with short hairpin RNA (shRNA; sh-TPI1) or a scrambled sequence (sh-NC), β-actin was used as an internal control. (b, c) WB analysis of TPI1, the EMT markers E-cadherin, N-cadherin, vimentin and Snail expressed in TPI1-silenced A549 and H1299 cells. β-actin served as an internal control. *$p < 0.05$, **$p < 0.01$, and ***$p < 0.001$. (d, e) Wound healing assays of cell migration in TPI1-silenced or control A549 and H1299 cells are as described in Figure 3d,e. *$p < 0.05$, **$p < 0.01$, and ***$p < 0.001$. (f, g) Migration and invasion abilities of TPI1-silenced A549 and H1299 cells were determined by transwell assays as described in Figure 3f,g.

cells. Initially, the gene expression data was categorized into two distinct groups based on the median expression level of TPI1: one with high expression and the other with low expression and the heatmap of differentially expressed genes (DEGs) is shown in Figure S1a. To ensure robustness, each analysis was subjected to 1000 permutations.

Throughout the entire analysis, the expression level of TPI1 was used as the defining phenotype. Subsequently, we categorized pathways exhibiting phenotypic enrichment based on both *p*-values and normalized enrichment scores (NESs). Our primary focus was on hallmark pathways, and the GSEA outcomes uncovered the enrichment of numerous gene sets within LUAD. Particularly noteworthy was the enrichment of gene sets related to EMT (Figure 5a), providing strong supporting evidence for our initial findings.

Concurrently, we performed GO analysis and Figure S1b–d showed the top 10 of GO biological processes (BP), GO cellular components (CC) and molecular functions. Meanwhile, our KEGG pathway enrichment analysis indicated that a significant proportion of differentially expressed genes were associated with the PI3K-Akt and MAPK signaling pathways (Figure 5b). Due to previous reports establishing a link between TPI1 and the PI3K-Akt pathway, we decided to shift our focus towards the MAPK signaling pathway. To validate our results, we proceeded to conduct a comprehensive analysis of the transcriptome data. The generation of a heatmap allowed us to identify proteins with fold changes within the MAPK signaling pathway, with the top 10 proteins emerging as hub genes in the pathway network (Figure 5c). Furthermore, we analyzed the differential mRNA expression of the top

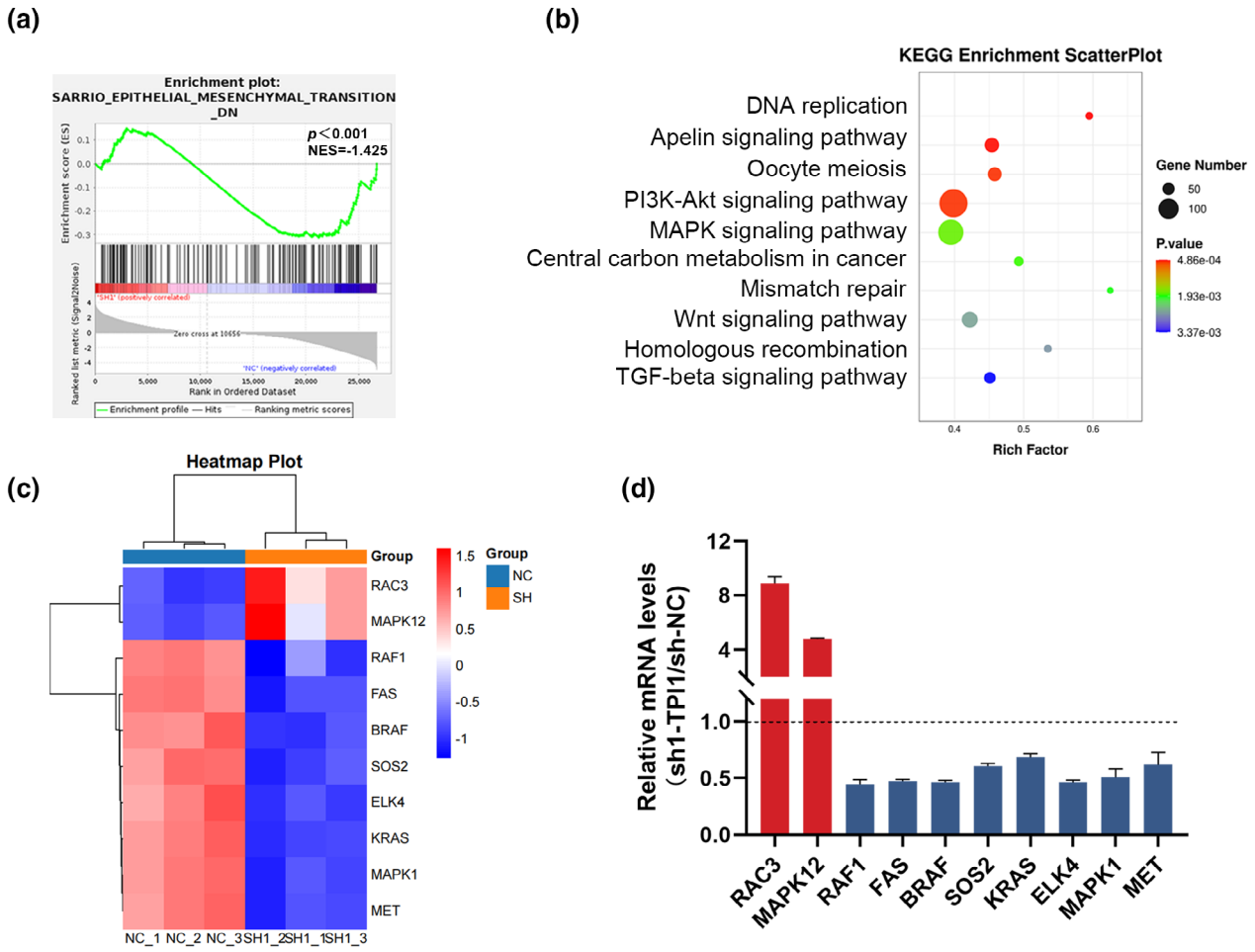

FIGURE 5 RNA-seq analysis of triosephosphate isomerase 1 (TPI1) associated with the mitogen-activated protein kinase (MAPK) signaling pathway. (a) Total RNA isolated from TPI1-silenced A549 cells was subjected to RNA-seq analysis as described in Methods. Gene set enrichment analysis (GSEA) of differentially expressed genes (DEGs) indicating an association of TPI1 with epithelial-mesenchymal transition (EMT). (b) Kyoto Encyclopedia of Genes and Genomes (KEGG) enrichment analysis showed the top 10 KEGG enrichment pathways. (c) Hierarchical cluster analysis (heatmap) was employed to show DEGs with a fold change of 1.5 or greater and a $q < 0.05$ in the MAPK signaling pathway. Three independent samples were tested in each group. Each column and row indicated a test sample and an mRNA, respectively. Red and blue denote high and low mRNA expression, respectively. (d) Quantitative reverse transcription- polymerase chain reaction (qRT-PCR) analysis of the mRNA expression of DEGs shown in Figure 5c, Data are shown as the mean ± SD ($n = 3$), TPI1-silenced A549 cells (sh-TPI1-1) compared to sh-NC by unpaired student's t-test. $^{*}p < 0.05$, $^{**}p < 0.01$, and $^{***}p < 0.001$.

10 hub genes in sh-TPI1-1 and sh-NC of A549 cells, and these findings were consistent with the heatmap results (Figure 5d).

TPI1 knockdown represses MAPK/ERK signaling-induced EMT of LUAD cells

Subsequently, in overexpressed-TPI1 A549 and H1299 cells, we investigated the p-ERK1/2, a downstream factor associated with the MAPK signaling pathway and its relevance to the EMT. Our findings showed that the overexpression of TPI1 led to a notable increase in ERK phosphorylation levels (Figure 6a). Furthermore, we employed PD98059 to inhibit the MAPK/ERK-mediated EMT, and the results demonstrated that the process of EMT induced by TPI1 overexpression was attenuated in the presence of PD98059 (Figure 6b).

In addition, we conducted a rescue experiment that involved both TPI1 knockdown and the activation of the ERK to assess p-ERK and EMT markers. We subjected silenced-TPI1 A549 and H1299 cells to EGF stimulation for 2 and 24 h. After a 2 h EGF stimulation, TPI1-silenced cells exhibited reduced levels of p-ERK compared to sh-NC cells. Subsequently, after a 24 h EGF stimulation, we observed E-cadherin increased and N-cadherin decreased (Figure 6c). Collectively, these results indicated TPI1 promotes MAPK/ERK-induced EMT and cell migration and invasion in LUAD.

DISCUSSION

Metabolism, under the regulation of metabolic enzymes, sustains cell growth and proliferation by supplying the

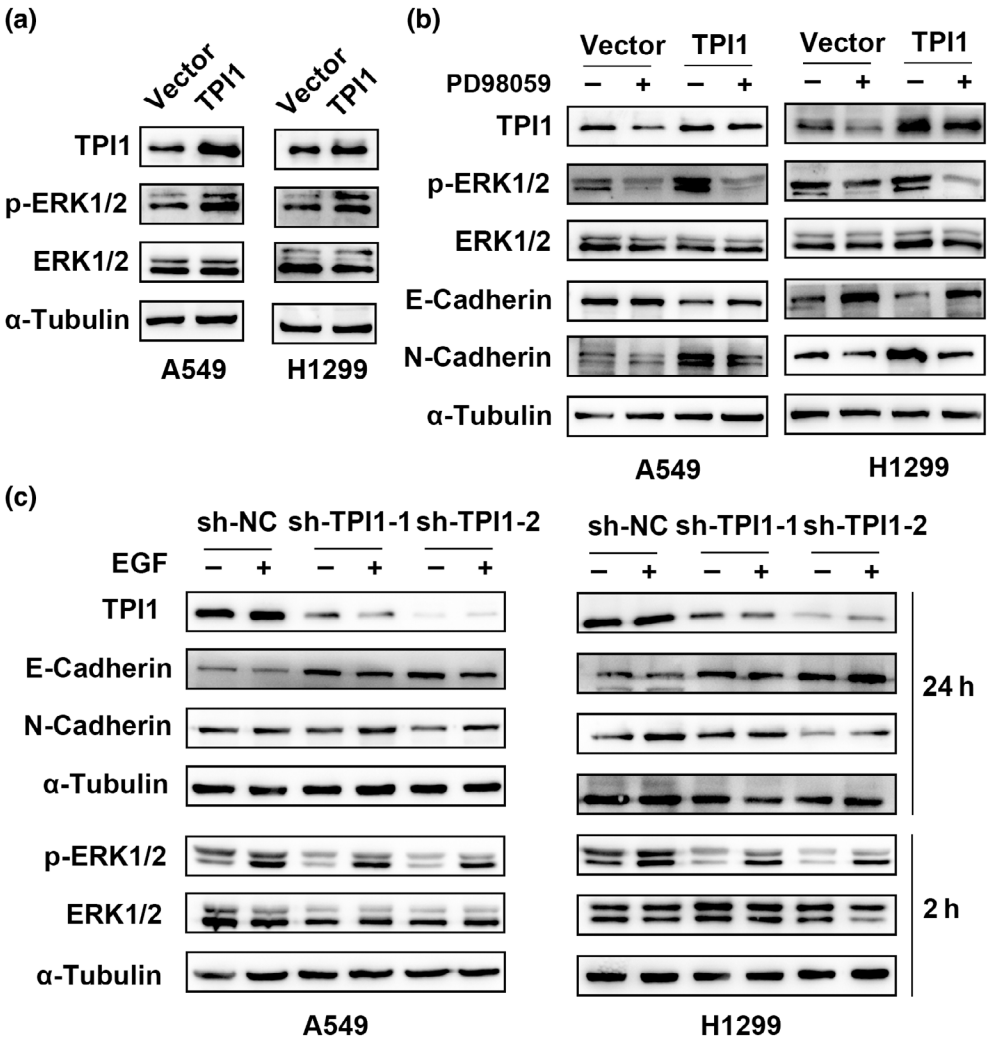

FIGURE 6 Triosephosphate isomerase 1 (TPI1) promotes epithelial-mesenchymal transition (EMT) of lung adenocarcinoma (LUAD) cells by upregulating the mitogen-activated protein kinase (MAPK)/extracellular regulated kinase (ERK) signaling pathway. (a) Western blot analysis of protein levels of TPI1, ERK, and p-ERK in TPI1-overexpressing A549 and H1299 cells. α-tubulin was used as an internal control. (b) TPI1-overexpressing or control A549 and H1299 cells were stimulated with or without PD98059 (20 μM) for 24 h. The expression of p-ERK, ERK, and EMT markers (E-cadherin and N-cadherin) were determined using Western blot. α-tubulin was used as an internal control. (c) TPI1-silenced or control A549 and H1299 cells were stimulated with or without epidermal growth factor (EGF) (50 ng/mL) for 2 h (upper panel) or 24 h (lower panel). The expression of p-ERK, ERK, and EMT markers (E-cadherin and N-cadherin) were determined using Western blot. α-tubulin was used as an internal control.

necessary energy for cellular processes.[26] Metabolic enzymes are the proteins responsible for catalyzing metabolic reactions.[27] Increasing evidence indicates that metabolic enzymes, beyond their primary role in catalyzing metabolic reactions, also perform diverse biological functions,[28] referred to as "moonlighting" functions.[29] Examples of this phenomenon include metabolic enzymes facilitating post-translational modifications like phosphorylation, acetylation,[30] and succinylation,[31] as well as influencing the subcellular localization of substrates, enabling them to engage directly in nonmetabolic processes.[32]

In our study, we noted elevated TPI1 expression across various tumor types. TPI1 catalyzes a reversible reaction between dihydroxyacetone phosphate and glyceraldehyde-3-phosphate. When glucose availability is low, dihydroxyacetone phosphate can be transformed into glyceraldehyde-3-phosphate to boost ATP production. However, the study by Yuan et al.[25] propose that even in the presence of ample glucose, inhibiting TPI1 does not impact glycolysis efficiency. This suggests that TPI1 promotes tumors through its nonmetabolic functions.

Utilizing bioinformatic methods, we found that TPI1 expression correlates with the TNM stage of tumors (Figure 2a). The T stage reflects the proliferation while the N and M stages indicate its metastatic potential.[33] Metastasis significantly contributes to the diminished 5-year survival rate in lung adenocarcinoma. Interestingly, we found that overexpression of TPI1 promotes the process of EMT, which may be one of the explanations for the higher rate of metastasis in patients with elevated TPI1 expression. Subsequently, we conducted KEGG enrichment analysis on RNA-seq data, revealing significant enrichment of the MAPK signaling pathway.

The MAPK signaling pathway consists of four classical branches: ERK, JNK, P38, and ERK5 and the MAPK/ERK pathway being documented as a key regulator of EMT.[11,12,34] Activation of this pathway initiates a phosphorylation cascade, starting with the phosphorylation of receptor tyrosine kinases (RTKs), which, in turn, activate the Ras protein. Activated Ras then triggers the Raf–MEK–ERK kinase cascade, ultimately leading to the phosphorylation and activation of ERK. Activated ERK translocates to the

nucleus, where it modulates the activity of various transcription factors, such as Snail, Slug, and Twist. These transcription factors, in turn, regulate the expression of genes involved in EMT, causing downregulation of epithelial markers such as E-cadherin and upregulation of mesenchymal markers such as N-cadherin and vimentin.[34–36] The overall effect is a phenotypic shift in cells from an epithelial to a mesenchymal state, promoting enhanced cellular motility, invasiveness, and metastatic potential.

To validate whether the TPI1/MAPK/ERK axis promotes EMT, PD98059 was used to block the MAPK/ERK signaling pathway,[37] and compared to the control group without inhibition, the decrease in E-cadherin and the increase in N-cadherin induced by overexpressing TPI1 were no longer significant. These results were similarly corroborated by activating the MAPK/ERK signaling pathway with EGF.

Unfortunately, the mechanisms by which TPI1 activates the MAPK/ERK signaling pathway remain unclear, and therefore deserve further exploration. Additionally, as seen in Figure 4f, PD98059 appeared to significantly reduce TPI1 expression. Current research suggests that PD98059 specifically inhibits the activity of MAPK/ERK kinases, thereby suppressing ERK1/2 phosphorylation and interfering with downstream signal transduction in the MAPK signaling pathway. Nevertheless, there have been no reports on the relationship between PD98059 and TPI1, which presents an intriguing avenue for future investigation.

The role of TPI1 in tumor development is indeed complex and remains incompletely understood. In some tumors, TPI1 expression is diminished (Figure 1a), exerting a tumor-suppressive effect. In our study, we reported the TPI1/MAPK/ERK axis as a driver of EMT, migration, and invasion in LUAD, contributing to a deeper comprehension of the mechanisms driving LUAD metastasis, and offering novel insights for potential treatment strategies in the future.

AUTHOR CONTRIBUTIONS

Conception and design, Yu Li and Chang Li. Administrative support, Bin Pan. Provision of study materials or patients, Feiyang Zhang and Xinyu Jia. Collection and assembly of data, Xinyu Zhu. Data analysis and interpretation, Xin Tong and Jun Zhao. All authors were responsible for writing the manuscript and its final approval.

FUNDING INFORMATION

This work was supported by the grants from National Natural Science Foundation of China (no. 81873417) and Soochow University Extracurricular Academic Research Fund (KY2023016Z).

CONFLICT OF INTEREST STATEMENT

The authors declare no conflicts of interest.

ORCID

Jun Zhao https://orcid.org/0000-0003-3846-8998
Chang Li https://orcid.org/0000-0002-9469-7173

REFERENCES

1. Sung H, Ferlay J, Siegel RL, Laversanne M, Soerjomataram I, Jemal A, et al. Global cancer statistics 2020: GLOBOCAN estimates of incidence and mortality worldwide for 36 cancers in 185 countries. CA Cancer J Clin. 2021;71(3):209–49.
2. Siegel RL, Miller KD, Fuchs HE, Jemal A. Cancer statistics, 2021. CA Cancer J Clin. 2021;71(1):7–33.
3. Howlader N, Forjaz G, Mooradian MJ, Meza R, Kong CY, Cronin KA, et al. The effect of advances in lung-cancer treatment on population mortality. N Engl J Med. 2020;383(7):640–9.
4. Gerstberger S, Jiang Q, Ganesh K. Metastasis. Cell. 2023;186(8):1564–79.
5. Chaffer CL, San Juan BP, Lim E, Weinberg RA. EMT, cell plasticity and metastasis. Cancer Metastasis Rev. 2016;35(4):645–54.
6. Steeg PS. Targeting metastasis. Nat Rev Cancer. 2016;16(4):201–18.
7. Pastushenko I, Blanpain C. EMT transition states during tumor progression and metastasis. Trends Cell Biol. 2019;29(3):212–26.
8. Peng D, Fu M, Wang M, Wei Y, Wei X. Targeting TGF-beta signal transduction for fibrosis and cancer therapy. Mol Cancer. 2022;21(1):104.
9. Lee JH, Massague J. TGF-beta in developmental and fibrogenic EMTs. Semin Cancer Biol. 2022;86(Pt 2):136–45.
10. Meurette O, Mehlen P. Notch signaling in the tumor microenvironment. Cancer Cell. 2018;34(4):536–48.
11. Chiu LY, Hsin IL, Yang TY, Sung WW, Chi JY, Chang JT, et al. The ERK-ZEB1 pathway mediates epithelial-mesenchymal transition in pemetrexed resistant lung cancer cells with suppression by vinca alkaloids. Oncogene. 2017;36(2):242–53.
12. Sheng W, Shi X, Lin Y, Tang J, Jia C, Cao R, et al. Musashi2 promotes EGF-induced EMT in pancreatic cancer via ZEB1-ERK/MAPK signaling. J Exp Clin Cancer Res. 2020;39(1):16.
13. Xu J, Wang Y, Jiang J, Yin C, Shi B. ADAM12 promotes clear cell renal cell carcinoma progression and triggers EMT via EGFR/ERK signaling pathway. J Transl Med. 2023;21(1):56.
14. Paul S, Ghosh S, Kumar S. Tumor glycolysis, an essential sweet tooth of tumor cells. Semin Cancer Biol. 2022;86(Pt 3):1216–30.
15. Ward PS, Thompson CB. Metabolic reprogramming: a cancer hallmark even Warburg did not anticipate. Cancer Cell. 2012;21(3):297–308.
16. Jin X, Wang D, Lei M, Guo Y, Cui Y, Chen F, et al. TPI1 activates the PI3K/AKT/mTOR signaling pathway to induce breast cancer progression by stabilizing CDCA5. J Transl Med. 2022;20(1):191.
17. Chen T, Huang Z, Tian Y, Wang H, Ouyang P, Chen H, et al. Role of triosephosphate isomerase and downstream functional genes on gastric cancer. Oncol Rep. 2017;38(3):1822–32.
18. Roth U, Razawi H, Hommer J, Engelmann K, Schwientek T, Müller S, et al. Differential expression proteomics of human colorectal cancer based on a syngeneic cellular model for the progression of adenoma to carcinoma. Proteomics. 2010;10(2):194–202.
19. Liu BHM, Tey SK, Mao X, Ma APY, Yeung CLS, Wong SWK, et al. TPI1-reduced extracellular vesicles mediated by Rab20 downregulation promotes aerobic glycolysis to drive hepatocarcinogenesis. J Extracell Vesicles. 2021;10(10):e12135.
20. Jiang H, Ma N, Shang Y, Zhou W, Chen T, Guan D, et al. Triosephosphate isomerase 1 suppresses growth, migration and invasion of hepatocellular carcinoma cells. Biochem Biophys Res Commun. 2017;482(4):1048–53.
21. Altenberg B, Greulich KO. Genes of glycolysis are ubiquitously overexpressed in 24 cancer classes. Genomics. 2004;84(6):1014–20.
22. Chin L, Andersen JN, Futreal PA. Cancer genomics: from discovery science to personalized medicine. Nat Med. 2011;17(3):297–303.
23. Kanehisa M, Furumichi M, Sato Y, Ishiguro-Watanabe M, Tanabe M. KEGG: integrating viruses and cellular organisms. Nucleic Acids Res. 2021;49(D1):D545–51.
24. Wu T, Hu E, Xu S, Chen M, Guo P, Dai Z, et al. clusterProfiler 4.0: a universal enrichment tool for interpreting omics data. Innovation (Camb). 2021;2(3):100141.

25. Liu P, Sun SJ, Ai YJ, Feng X, Zheng YM, Gao Y, et al. Elevated nuclear localization of glycolytic enzyme TPI1 promotes lung adenocarcinoma and enhances chemoresistance. Cell Death Dis. 2022;13(3):205.
26. Hsu PP, Sabatini DM. Cancer cell metabolism: Warburg and beyond. Cell. 2008;134(5):703–7.
27. Koppenol WH, Bounds PL, Dang CV. Otto Warburg's contributions to current concepts of cancer metabolism. Nat Rev Cancer. 2011; 11(5):325–37.
28. Lu S, Wang Y. Nonmetabolic functions of metabolic enzymes in cancer development. Cancer Commun (Lond). 2018;38(1):63.
29. Jiang J, Peng L, Wang K, Huang C. Moonlighting metabolic enzymes in cancer: new perspectives on the redox code. Antioxid Redox Signal. 2021;34(13):979–1003.
30. Kim SC, Sprung R, Chen Y, Xu Y, Ball H, Pei J, et al. Substrate and functional diversity of lysine acetylation revealed by a proteomics survey. Mol Cell. 2006;23(4):607–18.
31. Li FL, Liu JP, Bao RX, Yan GQ, Feng X, Xu YP, et al. Acetylation accumulates PFKFB3 in cytoplasm to promote glycolysis and protects cells from cisplatin-induced apoptosis. Nat Commun. 2018;9(1):508.
32. Yang W, Xia Y, Hawke D, Li X, Liang J, Xing D, et al. PKM2 phosphorylates histone H3 and promotes gene transcription and tumorigenesis. Cell. 2012;150(4):685–96.
33. Goldstraw P, Chansky K, Crowley J, Rami-Porta R, Asamura H, Eberhardt WEE, et al. The IASLC lung cancer staging project: proposals for revision of the TNM stage groupings in the forthcoming (eighth) edition of the TNM classification for lung cancer. J Thorac Oncol. 2016;11(1):39–51.
34. Ullah R, Yin Q, Snell AH, Wan L. RAF-MEK-ERK pathway in cancer evolution and treatment. Semin Cancer Biol. 2022;85:123–54.
35. Wang P, Jia X, Lu B, Huang H, Liu J, Liu X, et al. Erianin suppresses constitutive activation of MAPK signaling pathway by inhibition of CRAF and MEK1/2. Signal Transduct Target Ther. 2023;8(1):96.
36. Santarpia L, Lippman SM, El-Naggar AK. Targeting the MAPK-RAS-RAF signaling pathway in cancer therapy. Expert Opin Ther Targets. 2012;16(1):103–19.
37. Mekkawy AI, Naguib YW, Alhaj-Suliman SO, Wafa EI, Ebeid K, Acri T, et al. Paclitaxel anticancer activity is enhanced by the MEK 1/2 inhibitor PD98059 in vitro and by PD98059-loaded nanoparticles in BRAF(V600E) melanoma-bearing mice. Int J Pharm. 2021;606:120876.

SUPPORTING INFORMATION

Additional supporting information can be found online in the Supporting Information section at the end of this article.

How to cite this article: Li Y, Pan B, Zhang F, Jia X, Zhu X, Tong X, et al. TPI1 promotes MAPK/ERK-induced EMT, cell migration and invasion in lung adenocarcinoma. Thorac Cancer. 2024;15(4): 327–38. https://doi.org/10.1111/1759-7714.15196

APPENDIX A

TABLE A1

Case	Gender	Age	Stage	TNM
1	M	63	IA	T1N0M0
2	M	71	IA	T1N0M0
3	F	72	IIIA	T3N2M0
4	M	74	IA	T1N0M0
5	M	68	IB	T2N0M0
6	F	54	IA	T1N0M0
7	F	73	IB	T2N0M0
8	M	71	IIB	T2N1M0
9	M	61	IA	T1N0M0
10	M	63	IIIA	T2N2M0
11	F	80	IA	T1N0M0
12	M	70	IIIA	T1N2M0
13	F	59	IA	T1N0M0
14	F	64	IV	T4N0M1
15	M	82	IV	T3N2M0
16	M	63	IA	T1N0M0
17	F	67	IA	T1N0M0
18	M	58	IIIA	T2N2M0
19	F	74	IA	T1N0M0
20	M	70	IA	T1N1M0
21	M	63	IA	T1N0M0
22	M	74	IIIA	T4N1M0
23	F	71	IIB	T2N1M0
24	M	64	IB	T2N0M0
25	F	84	IA	T1N0M0
26	F	60	IIB	T2N1M0
27	M	51	IIB	T2N1M0
28	F	67	IA	T1N0M0
29	M	56	IA	T1N0M0

TABLE A2

Primer sequences	
Gene	**Sequence**
TPI1-F	CTCATCGGCACTCTGAACG
TPI1-R	GCGAAGTCGATATAGGCAGTAGG
FAS-F	TCTGGTTCTTACGTCTGTTGC
FAS-R	CTGTGCAGTCCCTAGCTTTCC
RAF1-F	GGGAGCTTGGAAGACGATCAG
RAF1-R	ACACGGATAGTGTTGCTTGTC
BRAF-F	AATACACCAGCAAGCTAGATGC
BRAF-R	AATCAGTTCCGTTCCCCAGAG
SOS2-F	CCGCAGCCTTACGAGTTCTTC
SOS2-R	GGATGCACTTGTTCCTGAACC
KRAS-F	ACAGAGAGTGGAGGATGCTTT
KRAS-R	TTTCACACAGCCAGGAGTCTT
ELK4-F	TGGACCTCTAATGATGGGCAG
ELK4-R	AGGCTTGTTCTTGCGAATCCC
MAPK1-F	TACACCAACCTCTCGTACATCG
MAPK1-R	CATGTCTGAAGCGCAGTAAGATT
MET-F	AGCAATGGGGAGTGTAAAGAGG
MET-R	CCCAGTCTTGTACTCAGCAAC
RAC3-F	TCCCCACCGTTTTTGACAACT
RAC3-R	GCACGAACATTCTCGAAGGAG
MAPK12-F	AGTGGCTTTTACCGCCAGG
MAPK12-R	GACTGGAAGGGCCGATACAG
ACTB-F	CATGTACGTTGCTATCCAGGC
ACTB-R	CTCCTTAATGTCACGCACGAT
ID	**Sequence**
sh-TPI1-1	CCGG-TGATGTGGATGGCTTCCTTGT-CTCGAG-ACAAGGAAGCCATCCACATCA-TTTTTT
Sh-TPI1-2	CCGG-CTCAGAGAGAAGGCATGTCTT-CTCGAG-AAGACATGCCTTCTCTCTGAG-TTTTTT